Energy and Momentum Growth Rates in Breaking Water Waves

Michael L. Banner and Xin Tian
School of Mathematics, University of New South Wales, Sydney 2052, Australia
(Received 20 May 1996)

Finding a parameter whose threshold controls the onset of breaking in nonlinear modulating surface gravity wave trains has been an elusive problem. Our numerical study of the fully nonlinear two-dimensional inviscid problem on a periodic spatial domain for a range of wave group structures examined the behavior of dimensionless relative growth rates of the local mean wave energy and momentum densities. We found that these growth rates at the envelope maxima of the wave group oscillate on a fast time scale with a significant dynamic range and that a universal threshold exists for the maximum of either of these growth rates that determines whether breaking will occur. [S0031-9007(96)01292-6]

PACS numbers: 47.35.+i, 47.20.Cq, 47.20.Ma

Ocean wind waves propagate in groups over the sea surface, with intermittent wave breaking occurring in the form of whitecaps at the maxima of the group envelopes. Despite the importance of wave breaking in both geophysical and offshore engineering applications, present understanding of its onset and consequences is very incomplete. Its mathematical counterpart, the prediction of wave breaking within modulating wave groups of nonlinear surface gravity waves, is a time honored and particularly challenging nonlinear free surface instability problem.

Previous efforts to find a breaking criterion in terms of a threshold of the local wave steepness, crest acceleration, or surface fluid velocity have been unsuccessful both from field observations and from computational models. Holthuijsen and Herbers [1] reported that it was almost impossible to distinguish the population of breaking waves at sea from the overall wave population on the basis of their slope probability distributions. A recent survey of previous investigations in Banner and Peregrine [2] and subsequent studies (e.g., [3–5]) further highlight the present lack of understanding of what determines whether breaking will occur within a modulating wave group.

The phenomenon is illustrated clearly by the computational wave examples shown in Fig. 1 where two wave groups with five waves in the modulation are shown at the top of each panel. They differ only marginally in the initial carrier wave slope $(ak)_0$. With initial slopes of 0.11 and 0.1125, respectively, the left and right side wave trains are both nonlinear. After about 250 carrier wave periods during the evolution, the two envelopes have deformed due to the nonlinearity and there is a pronounced local growth of the wave envelope. Later, at 535 and 440 carrier wave periods for the left and right panels, respectively, the dominant (largest amplitude) section of the wave envelope has grown larger at the expense of the amplitude of the other parts of the group. At this stage, the local steepness ak, the potential energy, and the vertical particle crest acceleration of the center wave in the left and right panels are virtually identical.

Subsequently, two distinct modes of behavior occur. The steepest wave in the left-hand side panel ceases to grow and then decreases in steepness as the wave train undergoes a recurrence towards the original group

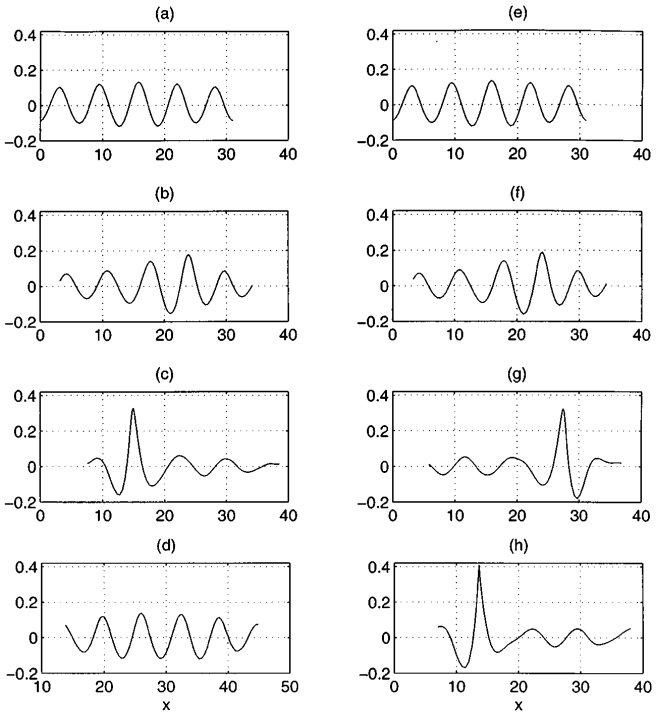

FIG. 1. Free surface profiles for an evolving wave group with five waves in one modulation. The initial group has a dominant center frequency and two small spectral sidebands. The left-hand panel (a)–(d) has initial slope $(ak)_0 = 0.11$ and shows evolution with recurrence. The associated times in wave periods are (a) $t = 0$, (b) $t = 80\pi$, (c) $t = 170\pi$, and (d) $t = 330\pi$. The right-hand panel (e)–(h) has $(ak)_0 = 0.1125$ and shows evolution to breaking. The evolution times in wave periods are (e) $t = 0$, (f) $t = 80\pi$, (g) $t = 140.2\pi$, and (h) $t = 149.8\pi$.

structure. The steepest wave in the right panel, with a comparable steepness, subsequently amplifies rapidly and evolves to breaking. The evolution process involves very strong spatial modulations in the local wave steepness as well as in the local propagation characteristics such as the wave number, frequency, and phase speed of the carrier waves.

This intriguing behavior was described previously by Dold and Peregrine [6] who reported results of their detailed computational model study of a fully nonlinear, two-dimensional, periodic domain free surface flow. They investigated the evolution of surface gravity wave trains that had small upper and lower sideband instabilities, using as parameters the initial carrier wave slope $(ak)_0$ and the number of waves in the group N, where $3 < N \leq 10$. They found a strong dependence of the wave train evolution on the parameter space $\{N, (ak)_0\}$. In particular, they determined a stability threshold curve for which breaking occurred above the indicated threshold, while below it a recurrence towards the original wave group ensued. The surprising aspect was the strong sensitivity of this stability threshold on N. Using their code, we reproduced the sensitivity of breaking onset to $\{N, (ak)_0\}$, but found that the actual slope at breaking varied only modestly for $3 < N \leq 10$ and showed no systematic dependence on N. This curious dependence of the initial slope of wave trains that ultimately break on the number of waves in the modulating group is one of many fascinating aspects of this problem that motivated the present effort to determine whether there exists an appropriate physical parameter with a "universal" threshold that controls the evolution to recurrence or breaking.

The carrier waves in a modulating wave group will grow if there are convergences of momentum flux and energy flux to a particular region of the group that on the average remain coherent with the group as it evolves under the influence of nonlinear interactions. In conservative systems, such sustained local convergences, arise through an exchange process with other regions within the wave group, leading to a corresponding reduction of their local energy or momentum density. If these local wave-coherent momentum and energy fluxes remain coherent with the growing part of the wave group for sufficiently long, the wave envelope will continue to grow and carrier waves passing through this region should evolve to break if the relative growth rates of the local mean wave momentum and energy densities are sufficiently large. Otherwise, the envelope may grow initially and then suddenly start to decay. Figure 1 illustrates these diverse scenarios.

To investigate the dynamics underlying a modulating wave group, we used the Dold-Peregrine free surface code (see Ref. [7] for details) to compute the evolution of the free surface in conjunction with our own code to generate the associated interior flow field. As the motion is irrotational, it is a potential flow and by Cauchy's integral theorem, the interior velocity field is determined at each time step by the boundary configuration.

From the interior flow field, at each time step we calculated the mean momentum density $\hat{M}(x,t)$ and mean energy density $\hat{E}(x,t)$. The local mean value is the spatial average taken over a suitable spatial distance, such as the local wavelength L, whose strong local modulation (see Fig. 1) needs to be carefully taken into account. When low-pass filtered, the Hilbert transform of the surface elevation yielded smoothed envelope and phase functions $A(x,t)$ and $\phi(x,t)$, respectively. Subsequent computation of $k = \partial\phi/\partial x$ and $\omega = -\partial\phi/\partial t$ provided accurate estimates of the distribution of local wave number k and frequency ω along the wave group. The wavelength-averaged local mean momentum density $\hat{M}$ is defined by $\hat{M}(x,t) = L^{-1}\int_{x-L/2}^{x+L/2}\int_{-d}^{\eta} u(x',y,t)dydx'$. Here x and y are the usual horizontal and vertical spatial coordinates, (u,v) is the velocity field, $y = \eta(x,t)$ is the free surface, d is the water depth (taken as several wavelengths), and $L(x,t)$ is the local wavelength. The water density is taken as unity. The wavelength-averaged local mean wave energy density along the group $\hat{E}$ is defined by $\hat{E}(x,t) = L^{-1}\int_{x-L/2}^{x+L/2}[\int_{-d}^{\eta}\frac{1}{2}(u^2+v^2)dy + \frac{1}{2}\eta^2]dx'$. Other localized mean momentum and energy densities were also found to the useful. These were based on half-wavelength averages, in which L is replaced by $L/2$ in these definitions. These averages are denoted by $\hat{M}_{1/2}(x,t)$ and $\hat{E}_{1/2}(x,t)$, respectively. Dimensionless growth rates $\beta_M(x,t)$ and $\beta_E(x,t)$ were then constructed for the relative growth rates of these locally averaged quantities as follows:

$$\beta_M = (\omega\hat{M})^{-1}D_*\hat{M}/Dt \text{ and } \beta_E = (\omega\hat{E})^{-1}D_*\hat{E}/Dt\,.$$

In these growth rate expressions, the derivative $D_*/Dt = \partial/\partial t + c_{\langle E \text{ or } M\rangle}\partial/\partial x$ is the derivative *following the envelope* of $\hat{E}(x,t)$ or $\hat{M}(x,t)$. Also, the local frequency ω varied along the wave group by up to 25%, but for the purpose of determining a breaking threshold parameter, it was more convenient to normalize by the constant linear mean carrier wave frequency. When rescaled by the true local frequency at the envelope maxima, the actual maximum relative growth rate is reduced by $O(25\%)$.

The major aim of the calculations carrier out in this study was to investigate the role of β_M and β_E as threshold variables to predict the onset of breaking in arbitrary modulating wave group situations. This required calculating the propagation characteristics of the associated envelopes. The envelope of $\hat{E}$ resulted directly as this quantity is positive definite, but that of $\hat{M}$ required calculation using the Hilbert transform. In the absence of explicit expressions, the speeds $c_{\langle E\rangle}$ and $c_{\langle M\rangle}$ of the peak of each envelope were computed from divided first differences of the horizontal displacement of the envelope peak at successive incremental time steps of 0.4π. Envelope propagation speeds for these

quantities were calculated for different stages of evolution of the nonlinear wave groups, both recurrent and breaking. The end result was that the behavior was consistently represented by taking $c_{\langle E\rangle} \sim c_{\langle M\rangle} \sim 0.75$ for both the full and half wavelength averages of both densities. The error incurred subsequently by taking this value as constant throughout the evolution was found to be insignificant in assessing the maximum value of the dimensionless growth rates.

For small slope, spatially uniform gravity wave trains, $\hat{E}$ and $\hat{M}$ have constant values of second order in the wave slope. For the unsteady, highly nonlinear wave groups in this study, $\hat{E}$ and $\hat{M}$ are still small quantities but are spatially nonuniform due to the strong local modulations that occur. Local mean energy and momentum densities along the wave group can become arbitrarily small, with the latter becoming negative. This behavior distorts the relative growth rates and was suppressed by applying lower bound thresholds. The physically relevant growth rates of the unstable section of the wave group were not affected by this process.

We validated the numerical procedures for the familiar test case of an infinitesimal slope wave group formed by the superposition of two slightly different wavelength, equal amplitude, infinitesimal slope wave trains with $(ak)_0 \sim 0.01$. Our computations reproduced the known results that when traveling with the linear *group velocity* ($c_{\langle E\rangle} \sim c_{\langle M\rangle} \sim 0.5$), the rate of change of $\hat{E}$ and $\hat{M}$ are zero at all locations along the group and hence $\beta_E(x,t) = \beta_M(x,t) = 0$ for all (x,t). For nonlinear modulating wave trains, we carefully examined the local behavior of $\hat{E}$, $\hat{M}$, $\hat{E}_{1/2}$, and $\hat{M}_{1/2}$ together with their rates of change following the velocity of their envelopes. Since the envelopes of $\hat{E}$ and $\hat{M}_{1/2}$ and their corresponding relative growth rates had a more compact distribution, these densities provided the most visual insight into the underlying dynamics and energetics. However, although less spatially compact, the other densities provided similar quantitative results for the growth rates.

This phase of the investigation led to fundamental new insights on the underlying instability process. It revealed the following for each of the densities: (a) The corresponding relative growth rate distribution $\beta_E(x,t)$ or $\beta_M(x,t)$ moves relative to the peak of the envelope of the quantity with a speed in excess of the envelope speed. This means that following the developing envelope, the envelope grows or decays on a slow time scale of $O(300)$ carrier wave periods on which is superimposed a small oscillatory component with a periodicity of $O(10)$ carrier wave periods. This complex behavior characterizes the evolution process of this very nonlinear system, both prior to the onset of breaking and during recurrence if breaking does not occur. Just prior to the onset of breaking, the growth becomes explosive. (b) The onset of breaking occurs if and only if the *maximum* value of the local oscillatory relative growth rate, $\beta^{\max}_{\langle E\rangle}$ or $\beta^{\max}_{\langle M\rangle}$, exceeds a certain threshold. This threshold appears to be universal. For this stage in the evolution, the local oscillatory character of the growth rate of the envelope maximum reduces markedly, the growth rate becomes more "phase locked" to the envelope maximum and the very rapid irreversible onset of breaking within $O(10\ \mathrm{T})$ ensues. Figure 2 shows the temporal evolution of $\beta^{\max}_{\langle E\rangle}$ and $\beta^{\max}_{\langle M\rangle}$ for the five-wave group shown in Fig. 1 for $\hat{M}_{1/2}$, $\hat{E}_{1/2}$, and $\hat{M}$. This evolution is typical of the many cases we examined in detail and for the whole parameter space $3 \le N \le 10$, the *same* threshold level of 0.2 was found for both half wavelength densities $\hat{M}_{1/2}$ and $\hat{E}_{1/2}$. The one wavelength average density $\hat{M}$ had a corresponding threshold value of 0.4 over the same parameter space.

We also investigated other initial modulating wave group configurations that might have a different evolution to breaking. For this we analyzed an initial wave group configuration with $N = 5$ but with a different initial condition comprising two equal spectral components of slope 0.07 and slightly different frequencies. For this case $(ak)_{\mathrm{breaking}}$ was 0.358, which is very similar to $(ak)_{\mathrm{breaking}}$ found for the case of the initial wave group with two small sidebands shown in Fig. 1. Also, previous studies (e.g., Refs. [8,9]) suggest a potentially strong influence of a linear surface shear on the evolution of wave groups. We extended our study to include surface shear currents typical of open ocean situations, using a constant linear shear profile of the form $U(y) = \Omega y$, with $y = 0$ at the mean water level. The effect of this surface shear layer was investigated for $N = 5$ and the initial wave group with two small spectral sidebands. The influence of shear reduced the slope at breaking

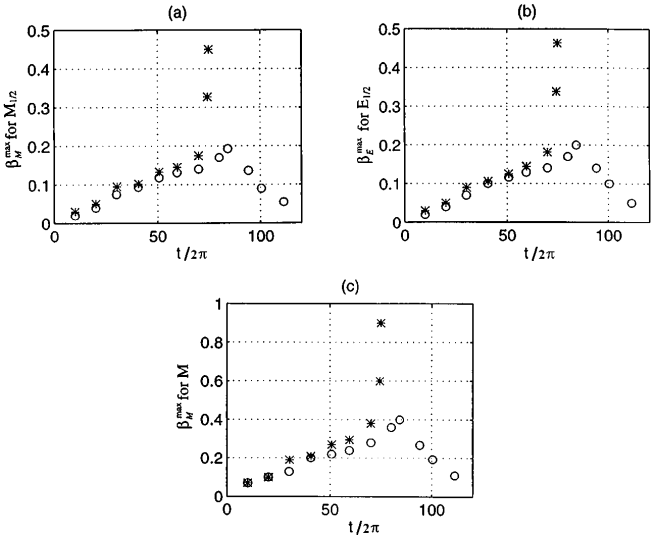

FIG. 2. Time evolution of the *maximum* growth rates $\beta^{\max}_{\langle E \text{ or } M\rangle}$ for the initial wave group configurations in Fig. 1 for (a) $\hat{M}_{1/2}$, (b) $\hat{E}_{1/2}$, and (c) $\hat{M}$. The symbol "o" shows the recurrent case, while "*" is the breaking case.

from 0.365 for the corresponding shear-free case of 0.306, a reduction of almost 20%. However, despite this significant change in the limiting carrier wave geometry, the maximum growth rates $\beta^{\max}_{\langle E \text{ or } M\rangle}$ for both of these different configurations coincided with the original group configuration result of 0.2 and 0.4, respectively, for the half and full wavelength-averaged densities.

In summary, we have elucidated the prediction of wave breaking in an unforced, inviscid, two-dimensional, nonlinear, modulating wave group. This has been formulated in terms of the behavior of the relative growth rates of the local mean energy and momentum, following the propagation speed of their envelopes. We have investigated different initial modulational configurations that lead to a significant range of local wave slopes at breaking, and have studied both irrotational and uniform background vorticity situations with vertical shear typical of ocean surface layer levels. The most significant findings are that within the constraints of the model the local growth rates of the envelope of the mean momentum and energy density have a fast oscillatory component superimposed on the longer term mean growth or decay. Whether breaking occurs during the longer-term evolution of the either of these quantities depends on a *universal* threshold based on the *maximum* value of these growth rate parameters: Breaking will occur if and only if at any stage of the evolution either $\beta^{\max}_{\langle E\rangle}(x,t)$ or $\beta^{\max}_{\langle M\rangle}(x,t)$ exceeds the value 0.2 for both $\hat{E}_{1/2}$ and $\hat{M}_{1/2}$, or equivalently 0.4 for the comparable full wavelength-averaged densities.

We note finally that applying the growth rate threshold criteria proposed here requires a detailed knowledge of the complete space-time structure of the subsurface flow field following the evolving wave group. We were unable to find an equivalent expression solely in terms of *free surface* variables.

We gratefully acknowledge the financial support of the Australian Research Council for this research project. We also sincerely thank our colleagues Professor D. H. Peregrine and Dr. J. W. Dold for allowing us to use their free surface code.

[1] L. H. Holthuijsen and T. H. C. Herbers, J. Phys. Oceanogr. **16**, 290 (1986).
[2] M. L. Banner and D. H. Peregrine, Ann. Rev. Fluid Mech. **25**, 373 (1993).
[3] W. W. Schultz, J. Huh, and O. M. Griffin, J. Fluid Mech. **278**, 301 (1994).
[4] M. P. Tulin and J. J. Li, J. Int. Soc. Offshore and Polar Eng. **2**, 46 (1992).
[5] P. Wang, Y. Yao, and M. P. Tulin, Proc. Third Int. Offshore and Polar Eng. Conf., Singapore **27** (1993).
[6] J. W. Dold and D. H. Peregrine, Proc. 20th. Int. Conf. Coastal Eng., Taipei, ASCE **163** (1986).
[7] J. W. Dold, J. Comp. Phys. **103**, 90 (1992).
[8] F. A. Millinazzo and P. G. Saffman, J. Fluid Mech. **216**, 93 (1990).
[9] A. F. Teles Da Silva and D. H. Peregrine, J. Fluid Mech. **195**, 281 (1988).